

*Electronic Supplementary Information*

**Photophysics of GFP-related Chromophores Imposed by a Scaffold Design**

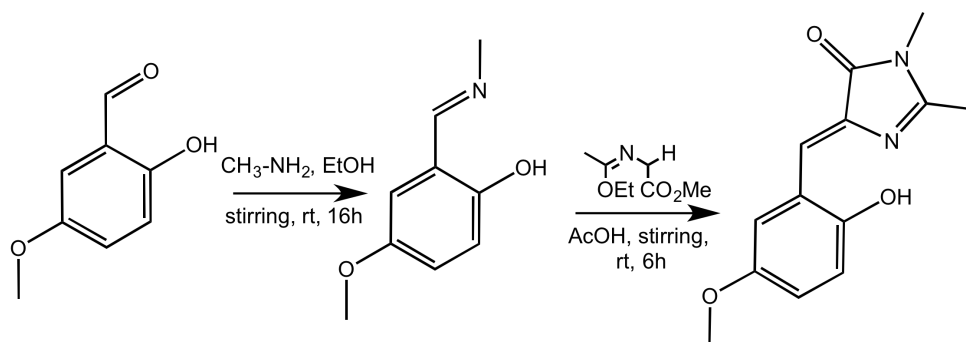
Ekaterina A. Dolgoplova, Thomas M. Moore, W. Brett Fellows, Mark D. Smith,  
Natalia B. Shustova\*

*Department of Chemistry and Biochemistry, University of South Carolina, Columbia, 29208,  
United States*

<b>Table of contents:</b>	<b>page number</b>
1. Synthesis of MeO- <i>o</i> HBI	<b>S2</b>
2. X-ray structure determination of <b>1</b> and MeO- <i>o</i> HBI	<b>S2</b>
3. <b>Table S1.</b> X-ray structure refinement data for <b>1</b> and MeO- <i>o</i> HBI	<b>S5</b>
4. <b>Figure S1.</b> X-ray crystal structure of <b>1</b>	<b>S6</b>
5. <b>Figure S2.</b> Simulated and experimental PXRD patterns of <b>1</b>	<b>S7</b>
6. <b>Figure S3.</b> Thermogravimetric analysis plot of <b>1</b>	<b>S8</b>
7. <b>Figure S4.</b> FT-IR spectrum of <b>1</b>	<b>S9</b>
8. <b>Figure S5.</b> PXRD patterns of <b>1</b> , BI@ <b>1</b> , <i>p</i> MBI@ <b>1</b> , HBI@ <b>1</b> , <i>o</i> HBI@ <b>1</b> , and MeO- <i>o</i> HBI@ <b>1</b>	<b>S10</b>
9. <b>Figure S6.</b> Normalized emission of MeO- <i>o</i> HBI in different solvents	<b>S11</b>
10. <b>Figure S7.</b> X-ray crystal structure of 5-(3-methoxybenzylidene)-2,3-dimethyl-3,5-dihydro-4 <i>H</i> -imidazol-4-one	<b>S12</b>
11. <b>Figure S8.</b> X-ray crystal structure of SBU of <b>2'</b> and <b>3</b>	<b>S13</b>
12. <b>Figure S9.</b> Simulated and experimental PXRD patterns of <b>2'</b>	<b>S14</b>
13. <b>Figure S10.</b> FT-IR spectrum of <b>2'</b>	<b>S15</b>
14. <b>Figure S11.</b> <sup>1</sup> H NMR and ESI MS spectra of digested <b>2'</b>	<b>S16</b>
15. <b>Figure S12.</b> Simulated and experimental PXRD patterns of <b>3</b>	<b>S17</b>
16. <b>Figure S13.</b> Thermogravimetric analysis plot of <b>3</b>	<b>S18</b>
17. <b>Figure S14.</b> FT-IR spectrum of <b>3</b>	<b>S19</b>
18. <b>Figure S15.</b> <sup>1</sup> H and <sup>13</sup> C NMR spectra of MeO- <i>o</i> HBI	<b>S20</b>
19. <b>Figure S16.</b> HBI wt% loading in <b>1</b> calculated from UV-vis calibration curve	<b>S21</b>
20. <b>References</b>	<b>S22</b>

**(Z)-5-(2-hydroxy-5-methoxybenzylidene)-2,3-dimethyl-3,5-dihydro-4H-imidazol-4-one (MeO-*o*HBI, Scheme 1).**

The MeO-*o*HBI chromophore was prepared by adaptation of the literature procedure.<sup>1</sup> A methylamine solution (33% in ethanol, 3.78 g, 40.2 mmol) was added to 2-hydroxy-5-methoxybenzaldehyde (0.610 g, 4.01 mmol), and the resulting solution was stirred for 16 h at room temperature. Methyl-2-((1-ethoxyethylidene)amino)acetate (0.830 g, 5.22 mmol) and a catalytic amount of acetic acid (40.0 mg, 0.700 mmol) were added after 16 h, and the resulting mixture was stirred vigorously for additional 6 h at room temperature. The obtained orange precipitate was collected by filtration and washed with water and diethyl ether. After drying under vacuum, MeO-*o*HBI (0.780 g, 3.17 mmol) was isolated in 79% yield. The NMR data match the reported spectra.<sup>2</sup> <sup>1</sup>H NMR (DMSO-*d*<sub>6</sub>, 300 MHz):  $\delta$  = 2.36 (3H, s), 3.11 (3H, s), 3.70 (3H, s), 6.80 (1H, d, *J* = 9 Hz), 6.91 (1H, dd, *J* = 9 Hz, 3 Hz), 7.22 (1H, s), 7.88 (1H, d, *J* = 3 Hz) (Figure S15). <sup>13</sup>C NMR (DMSO-*d*<sub>6</sub>, 400 MHz):  $\delta$  = 15.74, 26.87, 55.94, 117.46, 117.83, 119.72, 121.04, 122.17, 136.70, 152.37, 162.94, 169.35 (Figure S16). HRMS (ESI, *m/z*) calculated for C<sub>13</sub>H<sub>14</sub>N<sub>2</sub>O<sub>3</sub> [M+H]<sup>+</sup> 247.1083, found 247.1069. Single-crystal X-ray data of MeO-*o*HBI is shown in Table S1 and Figure 5.



**Scheme S1.** Synthesis of MeO-*o*HBI.

**X-ray Structure Determination.**

**Single-crystal X-ray structure of 1** (Zn<sub>6</sub>(BTC)<sub>4</sub>(H<sub>2</sub>O)<sub>3</sub>(DMF)<sub>3</sub>) 2(H<sub>2</sub>O)·4.7(DMF).

X-ray intensity data from a colorless prism were collected at 100(2) K using a Bruker D8 QUEST diffractometer equipped with a PHOTON 100 CMOS area detector and an Incoatec microfocus source (Mo K $\alpha$  radiation,  $\lambda$  = 0.71073 Å).<sup>3</sup> The raw area detector data frames were reduced and corrected for absorption effects using the SAINT+ and SADABS programs.<sup>3</sup> Final unit cell parameters were determined by least-squares refinement of 9322 reflections taken from the data set. The structure was solved by direct methods with SHELXT.<sup>4</sup> Subsequent difference Fourier calculations and full-matrix least-squares refinement against  $F^2$  were performed with SHELXL-2014<sup>4</sup> using OLEX2.<sup>5</sup>

The compound crystallizes in the cubic system. Indexing using the stronger reflections gave a face-centered cubic unit cell with  $a = 26.54 \text{ \AA}$ ,  $V = 18689 \text{ \AA}^3$ , consistent with the published data.<sup>6</sup> Careful examination of the diffraction pattern showed many weaker reflections with indices of *ca.* 0.5, suggesting a doubling of the cubic  $a$  axis. Indexing with these weaker data included gave a cubic cell with  $a = 53.077(2) \text{ \AA}$ ,  $V = 149530(18) \text{ \AA}^3$ , maintaining the face-centered Bravais lattice. Systematic absences in the intensity data were consistent the space groups  $F-43c$  and  $Fm-3c$ . The centrosymmetric group  $Fm-3c$  (No. 226) was determined by be correct. The asymmetric unit consists of three independent zinc atoms, two (Zn1 and Zn2) located on mirror planes and one (Zn3) located on a general position, one complete  $C_9H_3O_6$  ligand and 1/3 of another  $C_9H_3O_6$  ligand situated about a three-fold axis of rotation, two water molecules located on mirror planes (coordinated to Zn1 and Zn2) and a DMF molecule coordinated to Zn3. The  $Zn_2$  unit formed by Zn3 and its symmetry-equivalent is located on a two-fold axis. A very large region of essentially featureless interstitial electron density was observed in the framework cavities. These are presumably a disordered mixture of water and DMF. The contribution of the disordered solvents to the structure factors was removed using the solvent-masking method in OLEX2.<sup>7</sup> The solvent-accessible void volume was calculated to be  $80129.6 \text{ \AA}^3$  (53.6% of the total unit cell volume), equivalent to 13233 electrons per unit cell. All non-hydrogen atoms were refined with anisotropic displacement parameters. Enhanced rigid-bond restraints (RIGU) were applied to the nitrogen-methyl carbon bonds of the DMF molecule, and to the Zn1/Zn2-water oxygen bonds. Both coordinated solvent species are likely affected by minor disorder. Despite the large size of the structure, hydrogen atoms bonded to carbon could be located in difference maps; they were included as riding atoms in the final cycles. The water hydrogens could not be located and were not calculated. The largest residual electron density peak in the final difference map is  $0.73 \text{ e/\AA}^3$ , located  $1.07 \text{ \AA}$  from H15, consistent with minor DMF disorder.

For comparison, solution with the smaller cubic cell (space group  $Fm-3m$ )<sup>6</sup> gave better  $R$ -factors ( $R_1 = 0.0415$ ,  $wR_2 = 0.1218$  after solvent masking), but imposes disorder on the axially coordinated water and DMF molecules; the DMF molecules are not even resolvable. This solution gives one unique zinc center, effectively scrambling these axial ligands. The additional weaker reflections observed in the diffraction pattern of our crystal arise from ordering of the water and DMF ligands, with water coordinated exclusively to the Zn1/Zn2 unit and DMF to the Zn3/Zn3\* unit. The enlarged unit cell allows this solvent ordering to be resolved.

**MeO-*o*HBI** ( $C_{13}H_{14}N_2O_3$ ). X-ray intensity data from an orange block were collected at 100(2) K

using a Bruker D8 QUEST diffractometer equipped with a PHOTON 100 CMOS area detector and an Incoatec microfocus source (Mo  $K\alpha$  radiation,  $\lambda = 0.71073 \text{ \AA}$ ).<sup>3</sup> The raw area detector data frames were reduced and corrected for absorption effects using the SAINT+ and SADABS programs.<sup>3</sup> Final unit cell parameters were determined by least-squares refinement of 9931 reflections taken from the data set. The structure was solved by direct methods with SHELXT.<sup>4</sup> Subsequent difference Fourier calculations and full-matrix least-squares refinement against  $F^2$  were performed with SHELXL-2014<sup>4</sup> using OLEX2.<sup>5</sup>

The compound crystallizes in the orthorhombic system. Intensity statistics indicated an acentric structure. The pattern of systematic absences in the intensity data was consistent with the space groups  $Pnma$  and  $Pna2_1$ , the latter of which was confirmed by structure solution. The finished refinement was checked for missed symmetry using the ADDSYM program in PLATON, which found none.<sup>7–10</sup> The asymmetric unit consists of one molecule. All non-hydrogen atoms were refined with anisotropic displacement parameters. Hydrogen atoms bonded to carbon were located in difference maps before being included as standard riding atoms. The hydroxyl hydrogen H2 was located in a difference map and refined freely. The largest residual electron density peak in the final difference map is  $0.35 \text{ e/\AA}^3$ , located  $0.69 \text{ \AA}$  from C8. Because of the absence of heavy atoms in the crystal, the absolute structure could not be reliably determined; however the Flack parameter<sup>11</sup> at convergence was  $0.02(18)$ , suggesting the correct orientation of the polar axis has been assigned.



**Table S1.** X-ray structure refinement data for **1<sup>a</sup>** and MeO-*o*HBI<sup>a</sup>.

compound	<b>1</b>	<b>MeO-<i>o</i>HBI</b>
formula	Zn <sub>6</sub> C <sub>45</sub> H <sub>39</sub> N <sub>3</sub> O <sub>30</sub> <sup>b</sup>	C <sub>13</sub> H <sub>14</sub> N <sub>2</sub> O <sub>3</sub>
FW	1494.01	246.26
<i>T</i> , K	100(2)	100(2)
crystal system	cubic	orthorombic
space group	Fm-3c	Pna2 <sub>1</sub>
<i>Z</i>	64	4
<i>a</i> , Å	53.077(2)	13.5916(8)
<i>b</i> , Å	53.077(2)	11.5913(7)
<i>c</i> , Å	53.077(2)	7.3557(4)
$\alpha$ , °	90	90
$\beta$ , °	90	90
$\gamma$ , °	90	90
<i>V</i> , Å <sup>3</sup>	149530(18)	1158.85(12)
<i>d</i> <sub>calc</sub> , g/cm <sup>3</sup>	1.062	1.411
$\mu$ , mm <sup>-1</sup>	1.572	0.102
F(000)	48000.0	520.0
crystal size, mm <sup>3</sup>	0.2×0.18× 0.14	0.48×0.4× 0.18
theta range	4.342 to 51.378	4.618 to 60.126
index ranges	−64 ≤ <i>h</i> ≤ 64 −63 ≤ <i>k</i> ≤ 63 −64 ≤ <i>l</i> ≤ 64	−19 ≤ <i>h</i> ≤ 19 −16 ≤ <i>k</i> ≤ 16 −10 ≤ <i>l</i> ≤ 10
refl. collected	422725	26712
data/restraints/ parameters	6149/32/255	3398/1/171
GOF on F <sup>2</sup>	1.065	1.064
Largest peak/ hole, e/Å <sup>3</sup>	0.73/−0.51	0.35/−0.27
R <sub>1</sub> /wR <sub>2</sub> , [ <i>I</i> ≥ 2σ( <i>I</i> )] <sup>c</sup>	0.0709/0.2086	0.0334/0.0913

<sup>a</sup> Mo-K $\alpha$  ( $\lambda$  = 0.71073 Å) radiation<sup>b</sup> Formula is given based on single-crystal X-ray data and does not include disordered solvent molecules (complete formula was determined based on the elemental analysis)<sup>c</sup>  $R_1 = \Sigma ||F_o| - |F_c|| / \Sigma |F_o|$ ,  $wR_2 = \{\Sigma [w(F_o^2 - F_c^2)^2] / \Sigma [w(F_o^2)^2]\}^{1/2}$

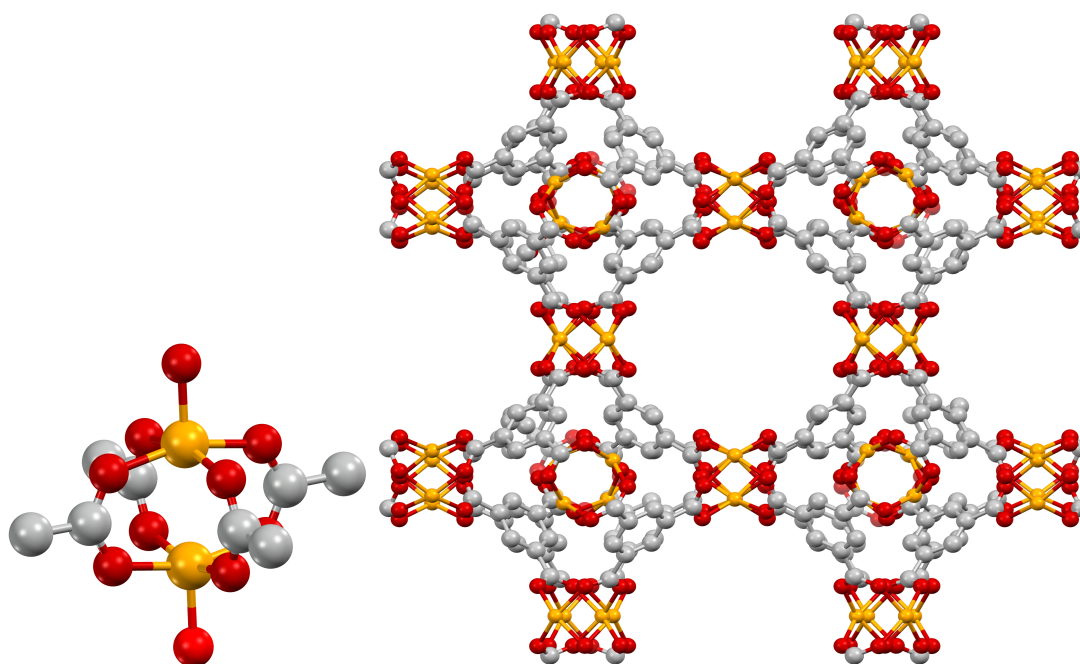


**Figure S1.** (*left*) The  $\text{Zn}_2(\text{O}_2\text{C})_4$  secondary building unit in **1**. (*right*) A part of the X-ray crystal structure of **1**. Orange, red and grey spheres represent Zn, O, and C atoms, respectively. Hydrogen atoms are omitted for clarity.

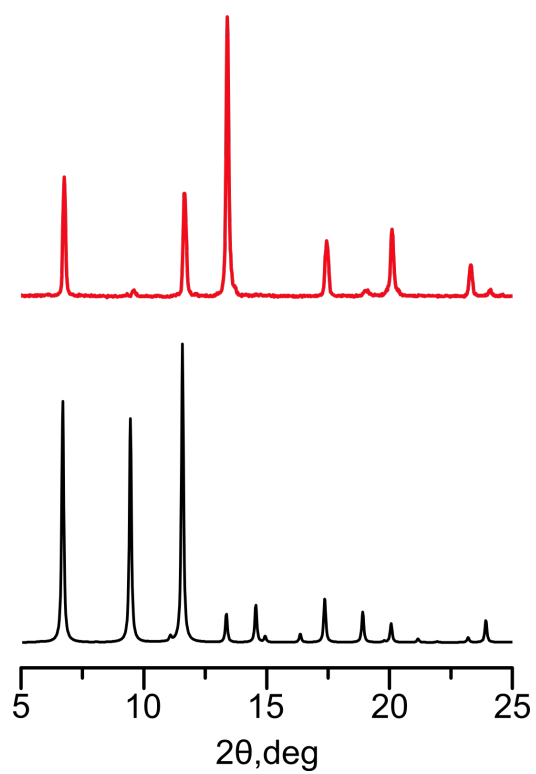


**Figure S2.** PXRD patterns of simulated (—) and as-synthesized (—) **1** with preferential orientation along the 001 direction.

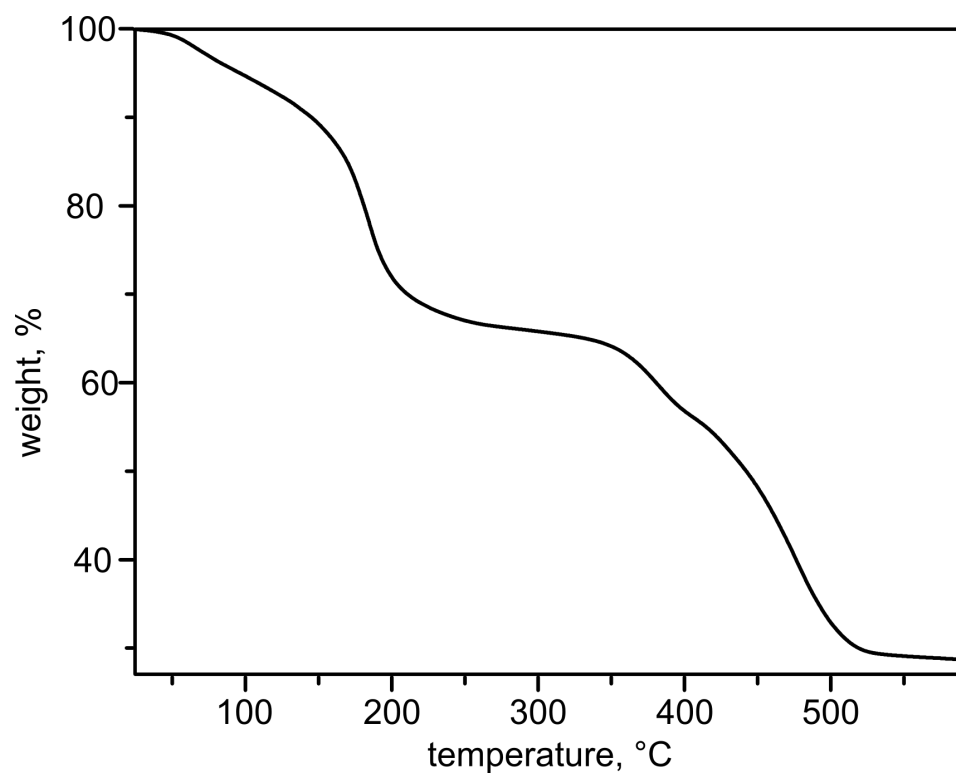


**Figure S3.** Thermogravimetric analysis plot of **1**.

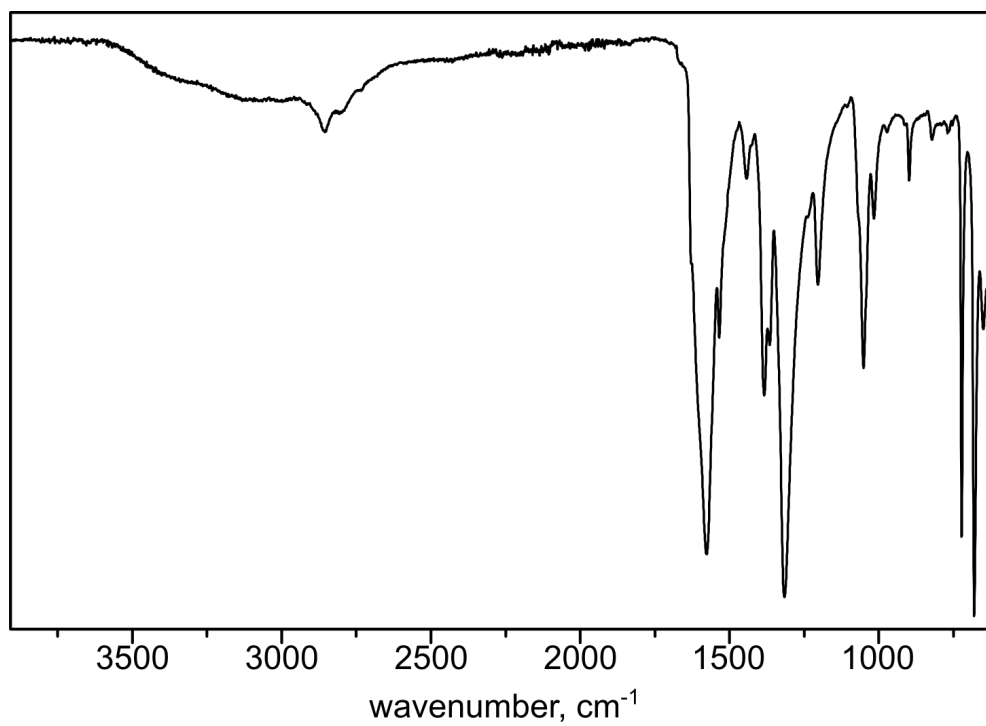


**Figure S4.** FT-IR spectrum of **1**.

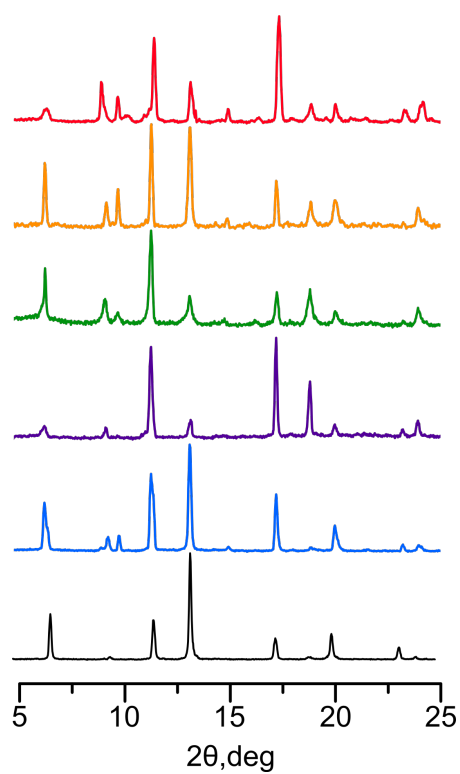


**Figure S5.** PXRD patterns of **1** (black), BI@**1** (blue), *p*MBI@**1** (purple), HBI@**1** (green), *o*HBI@**1** (orange), and MeO-*o*HBI@**1** (red).

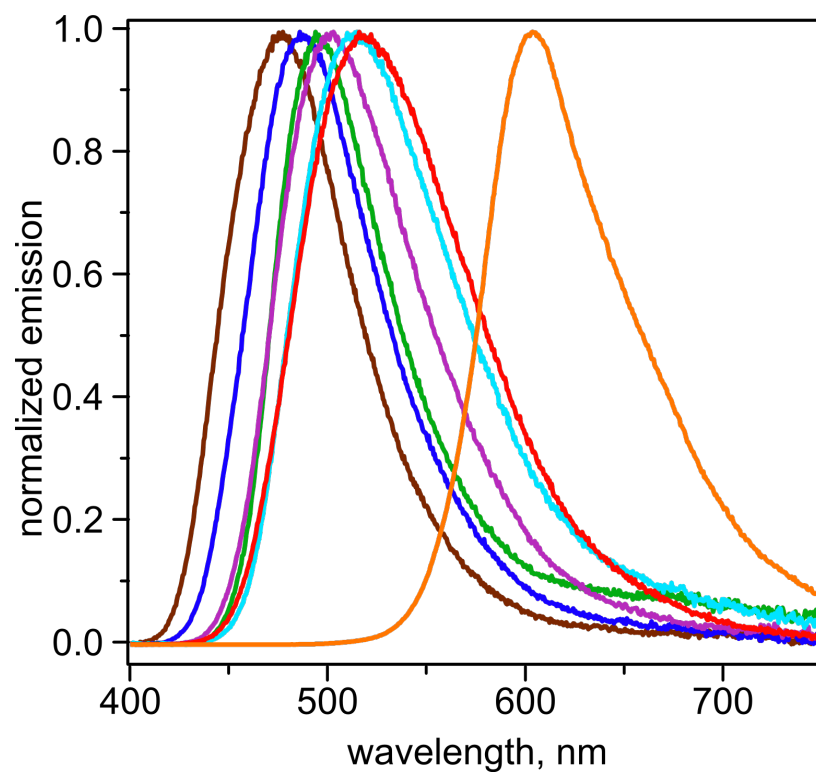


**Figure S6.** Normalized emission ( $\lambda_{\text{ex}} = 360$  nm) of MeO-*o*HBI in diethyl ether (brown), tetrahydrofuran (blue), ethyl acetate (green), acetone (purple), acetonitrile (cyan), *N,N*-dimethylformamide (red), and in the solid state (orange).

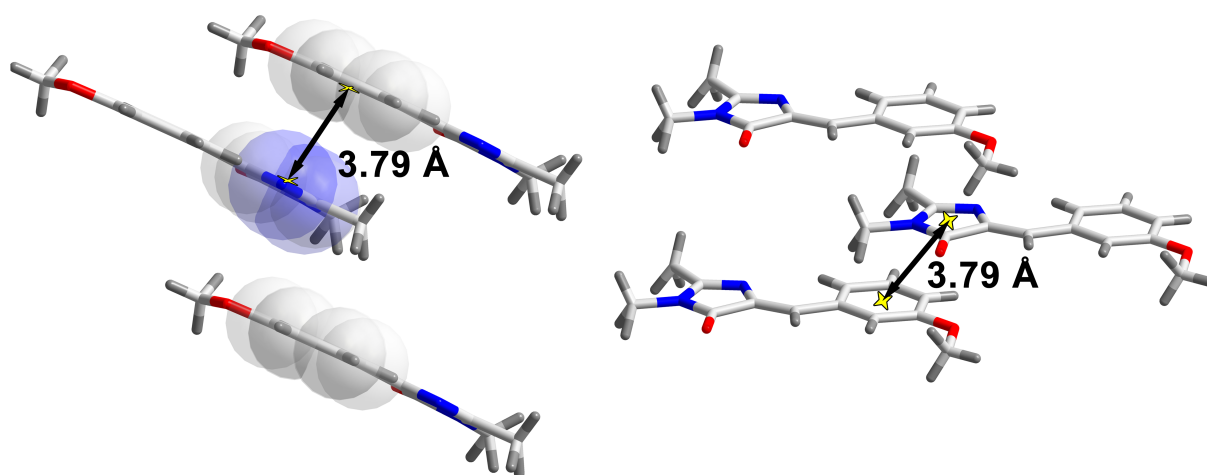


**Figure S7.** Two views of packing of 5-(3-methoxybenzylidene)-2,3-dimethyl-3,5-dihydro-4*H*-imidazol-4-one.<sup>12</sup> The distance between centroids of phenyl and imidazolinone rings is 3.79 Å.



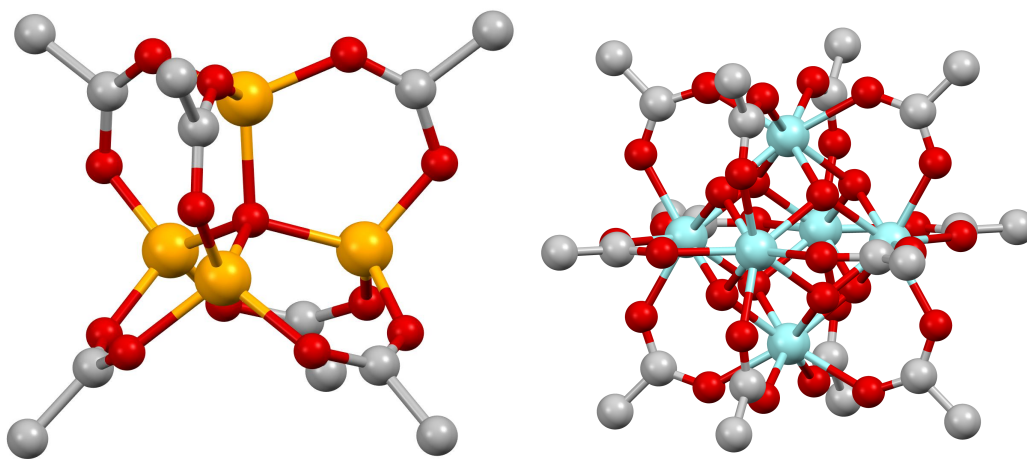


**Figure S8.** (*left*) The  $\text{Zn}_4\text{O}(\text{O}_2\text{C}-)_6$  secondary building unit in **2** (isoreticular to prepared **2'**).<sup>13</sup> (*right*) The  $\text{Zr}_6\text{O}_4(\text{OH})_4$  secondary building unit in UIO-67 (isoreticular to prepared **3**).<sup>14</sup> Orange, blue, red, and grey spheres represent Zn, Zr, O, and C atoms, respectively. Hydrogen atoms are omitted for clarity.

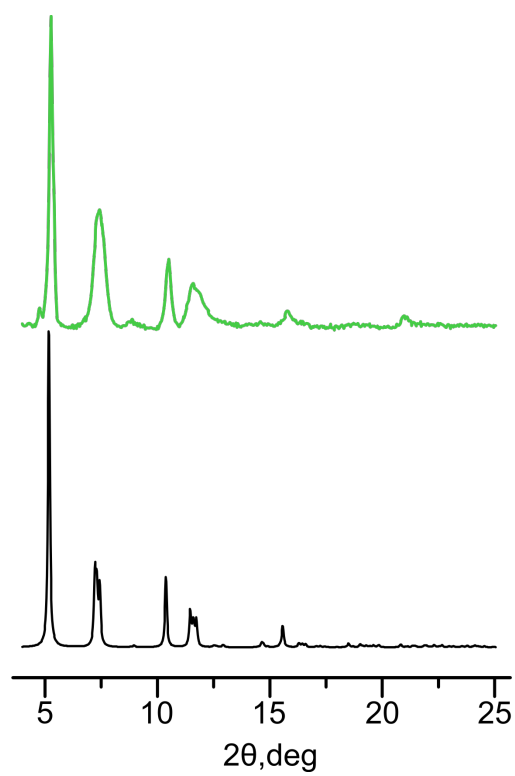


**Figure S9.** PXRD patterns of simulated (—) and as-synthesized (—) **2'**.

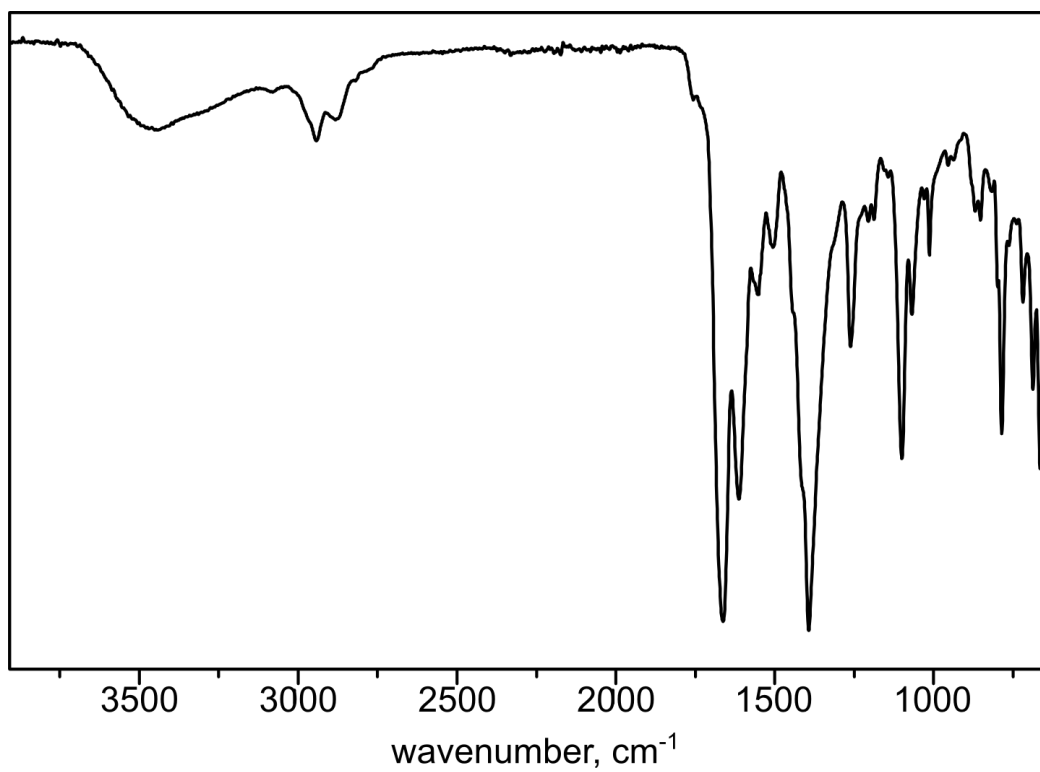


**Figure S10.** FT-IR spectrum of **2'**.

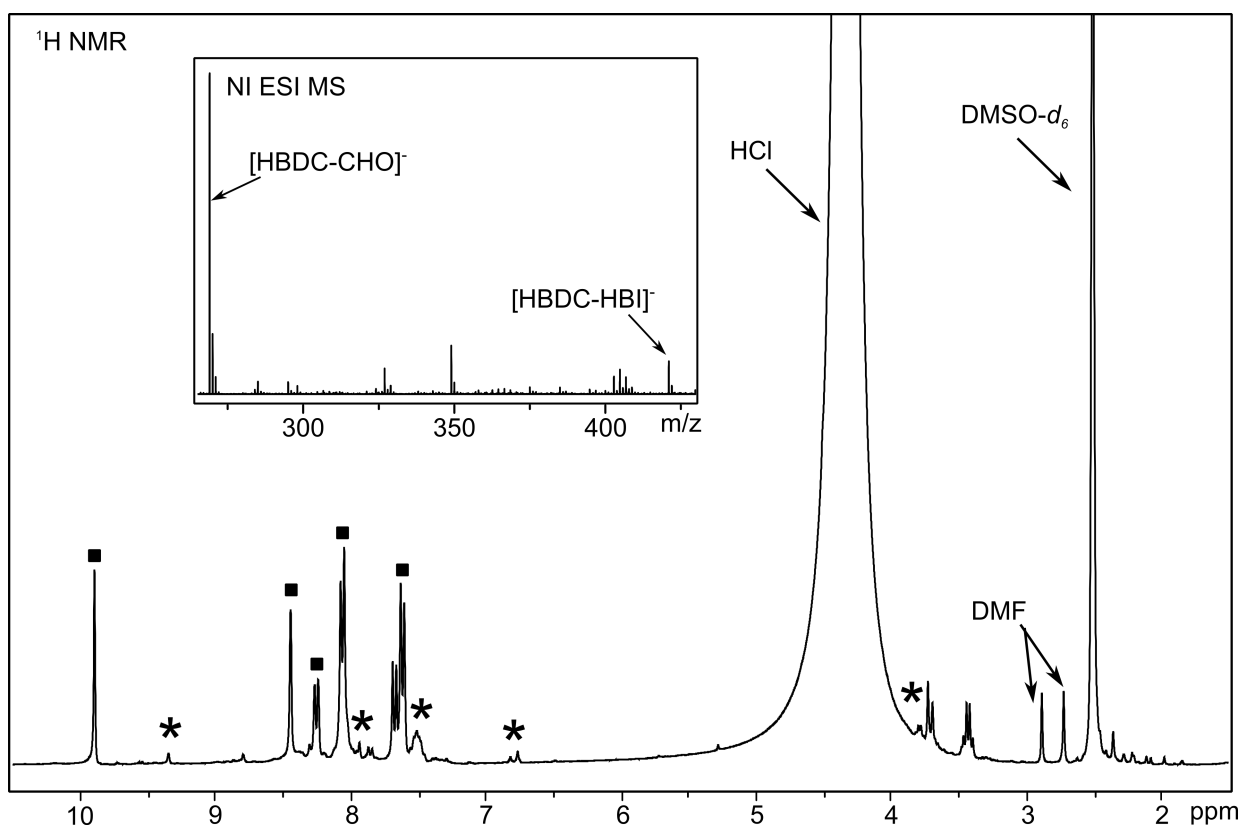


**Figure S11.**  $^1\text{H}$  NMR spectrum of digested **2'** in  $\text{DMSO-}d_6$ . The inset shows the negative ion electrospray ionization mass-spectrum (NI ESI MS) of digested **2'**. The peaks corresponding to  $\text{H}_2\text{BDC-CHO}$  (■) and  $\text{H}_2\text{BDC-BI}$  (\*) are labeled.

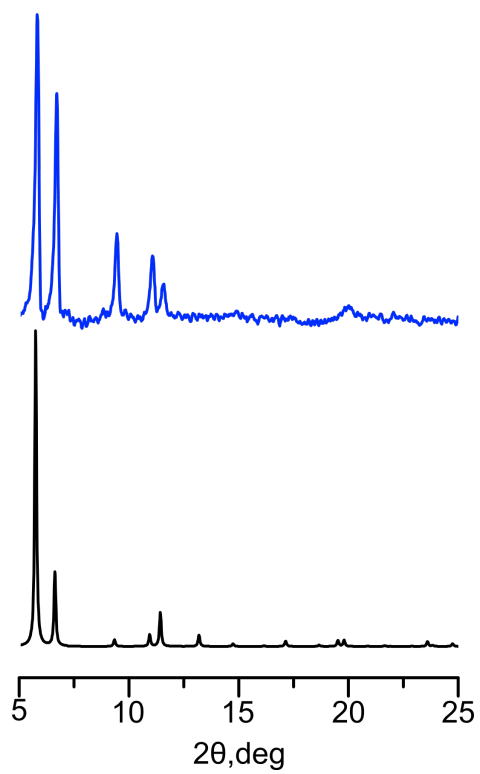


**Figure S12.** PXRD patterns of simulated (—) and as-synthesized (—) **3**.

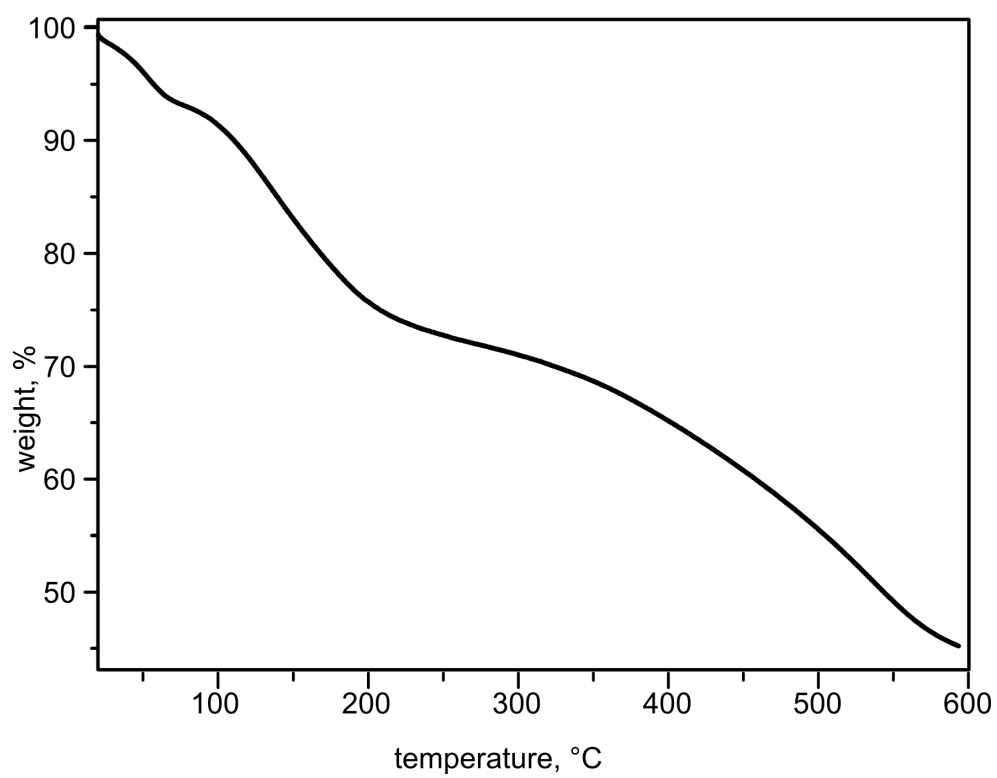


**Figure S13.** Thermogravimetric analysis plot of **3**.

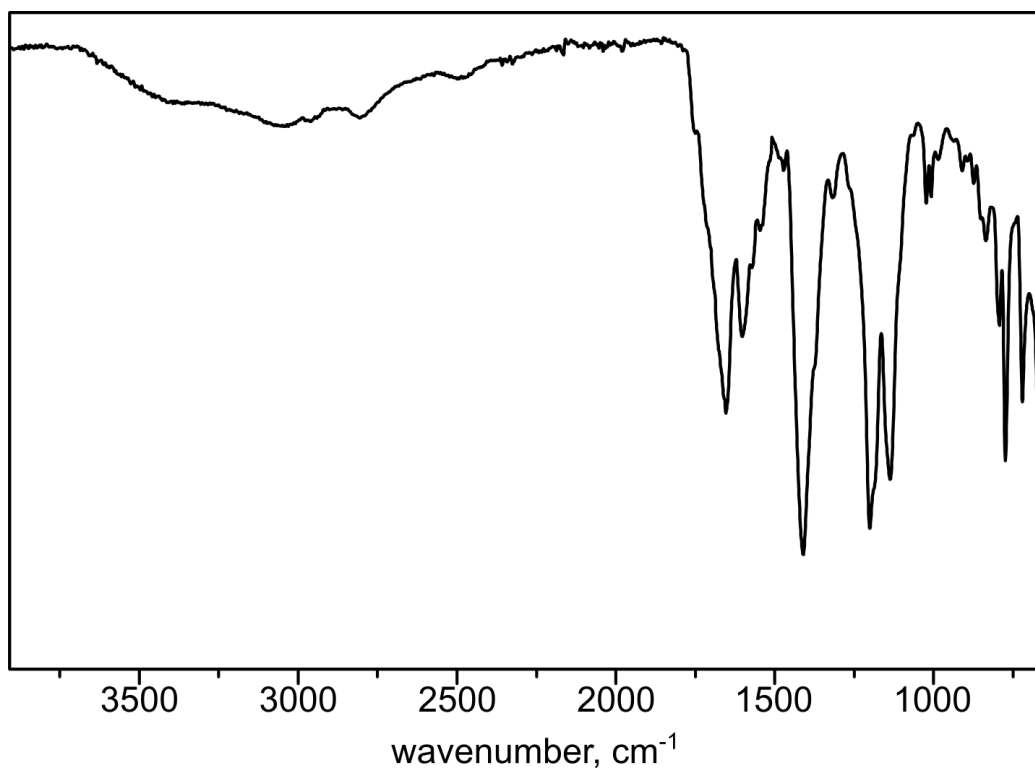


**Figure S14.** FT-IR spectrum of **3**.

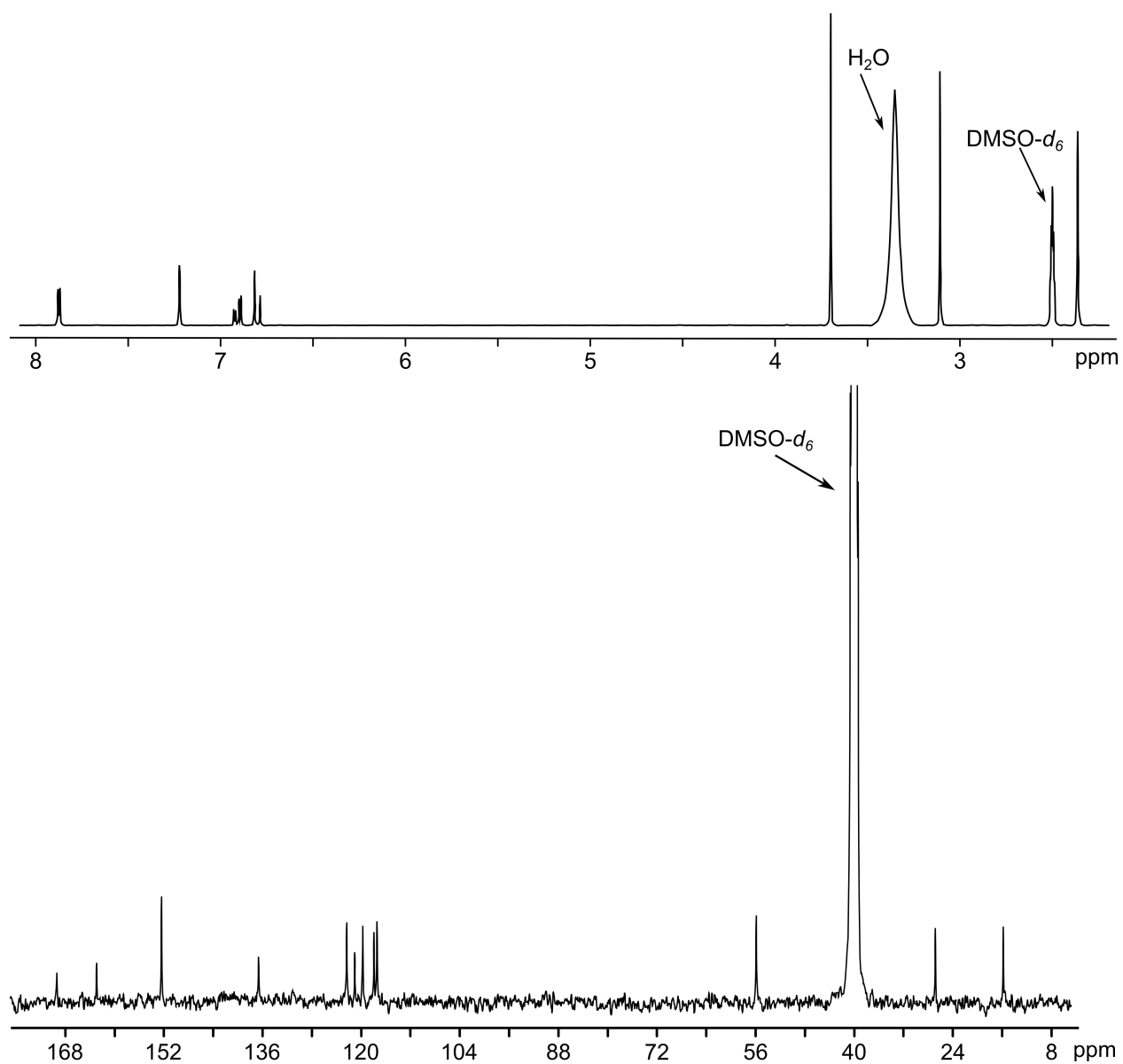


**Figure S15.**  $^1\text{H}$  NMR (top) and  $^{13}\text{C}$  NMR (bottom) spectra of synthesized MeO-*o*HBI.



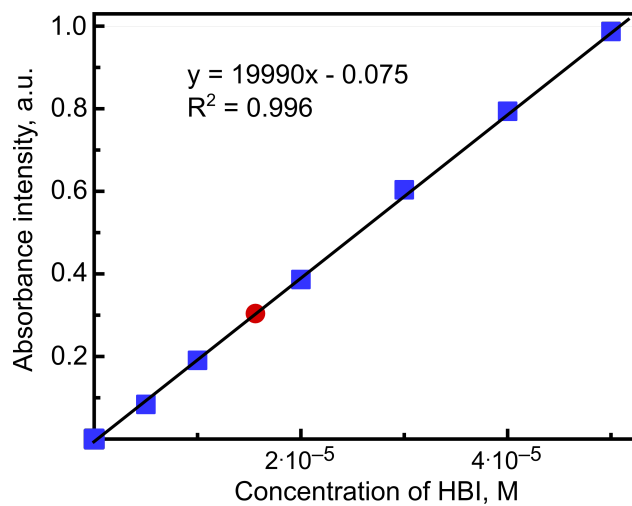


**Figure S16.** HBI loading (wt%) in **1** calculated from the UV-vis calibration curve.

## References:

- 1 A. Baldrige, J. Kowalik and L. M. Tolbert, *Synthesis*, 2010, **14**, 2424–2436.
- 2 W.-T. Chuang, C.-C. Hsieh, C.-H. Lai, C.-H. Lai, C.-W. Shih, K.-Y. Chen, W.-Y. Hung, Y.-H. Hsu and P.-T. Chou, *J. Org. Chem.*, 2011, **76**, 8189–8202.
- 3 Bruker, *APEX II*, 2014, Bruker AXS Inc., Madison, Wisconsin, USA.
- 4 G. M. Sheldrick, *Acta Cryst.*, 2008, **A64**, 112–122.
- 5 O. V. Dolomanov, L. J. Bourhis, R. J. Gildea, J. A. K. Howard and H. Puschmann, *J. Appl. Cryst.*, 2009, **42**, 339–341.
- 6 X. Song, S. Jeong, D. Kim and M. S. Lah, *CrystEngComm*, 2012, **14**, 5753–5756.
- 7 P. van der Sluis and A. L. Spek, *Acta Cryst.*, 1990, **A46**, 194–201.
- 8 Y. Le Page, *J. Appl. Cryst.*, 1987, **20**, 264–269.
- 9 A. L. Spek, *Acta Cryst.*, 1990, **A46**, 34.
- 10 A. L. Spek, *J. Appl. Cryst.*, 1988, **21**, 578–579.
- 11 S. Parsons, H. D. Flack and T. Wagner, *Acta Cryst.*, 2013, **B69**, 249–259.
- 12 P. Naumov, J. Kowalik, K. M. Solntsev, A. Baldrige, J.-S. Moon, C. Kranz and L. M. Tolbert, *J. Am. Chem. Soc.*, 2010, **132**, 5845–5857.
- 13 D. E. Williams, E. A. Dolgoplova, P. J. Pellechia, A. Palukoshka, T. J. Wilson, R. Tan, J. M. Maier, A. B. Greytak, M. D. Smith, J. A. Krause and N. B. Shustova, *J. Am. Chem. Soc.*, 2015, **137**, 2223–2226.
- 14 G. Nickerl, M. Leistner, S. Helten, V. Bon, I. Senkovska and S. Kaskel, *Inorg. Chem. Front.*, 2014, **1**, 325–330.